In situ FTIR study of cobalt oxides for the oxidation of carbon monoxide

Hung-Kuan Lin [a,b], Chen-Bin Wang [a,*], Hui-Chi Chiu [b], and Shu-Hua Chien [b,c,*]

[a] *Department of Applied Chemistry, Chung Cheng Institute of Technology, National Defense University, Tahsi, Taoyuan 33509, Taiwan, Republic of China*

[b] *Institute of Chemistry, Academia Sinica, Taipei 11529, Taiwan, Republic of China*

[c] *Department of Chemistry, National Taiwan University, Taipei 10764, Taiwan, Republic of China*

Received 5 September 2002; accepted 14 November 2002

A high-valance cobalt oxide, CoO_x, was prepared from cobalt nitrate aqueous solution through precipitation with sodium hydroxide and oxidation by hydrogen peroxide. Further, other pure cobalt oxide species were refined from the CoO_x by temperature-programmed reduction (TPR) to 170, 230 and 300 °C. They were characterized by TPR and X-ray diffraction (XRD). Adsorption of CO and the co-adsorption of CO/O_2 over the cobalt oxides were further tested by *in situ* FTIR. It was shown that Co_3O_4 is quite active for the oxidation of CO at room temperature in the presence of oxygen, leading to the formation of CO_2. The variation in the oxidation of CO was interpreted with a mechanism involving two kinds of oxygen species, i.e., $*–O_2$ on the CoO_x surface and $*–O_L$ on the surface of Co_3O_4 spinel structure.

KEY WORDS: cobalt oxide; FTIR; CO oxidation; adsorption.

1. Introduction

Cobalt oxide, as an important catalyst for complete oxidation [1], is one of the most versatile materials among the transition metal oxides. Unsupported cobalt oxide is a very active species in the field of air pollution control of CO [2–6] and NO_x [7–9] and for the control of organic pollutants from effluent streams [10,11]. Also, cobalt oxide is important for the development of rechargeable batteries [12–14] and CO sensors [4,15–17].

It is known that Co_3O_4 and CoO are stable oxides among the cobalt oxide systems [18,19]. However, a valence of cobalt higher than +3 is thermally unstable. Some reports [20–23] have described special methods to obtain the higher cobalt oxides Co_2O_3 and CoO_2. Zee *et al.* [20] used a laser technique to vaporize cobalt metal under oxygen that obtained CoO_2. Based on the electrochemical deposition method, Co_2O_3 was obtained by Elemongy *et al.* [21] and Yih-Wen and Rommel [22]. The higher cobalt oxide was obtained by Christoskova *et al.* [23] using the precipitation–oxidation process in a sodium hypochlorite aqueous solution, although chloride ion contamination could not be avoided.

In an attempt to improve the control of the preparation of high-valence cobalt oxide and to avoid possible contamination, we apply the precipitation–oxidation method and use hydrogen peroxide as oxidant. A series of pure cobalt oxide species are further refined from the high-valence cobalt oxide by the temperature-programmed reduction (TPR) technique. This work aims to characterize these oxides and to investigate, using *in situ* FTIR, the cobalt oxides in CO and CO/O_2, in an attempt to elucidate the nature of the catalytic active sites for CO oxidation.

* To whom correspondence should be addressed.
E-mail: chenbin@ccit.edu.tw; chiensh@gate.sinica.edu.tw

2. Experimental

2.1. Sample preparation

The crude cobalt oxide (CoO_x) with high-valence cobalt was synthesized by the precipitation–oxidation method in an aqueous solution. The precipitation process was carried out at 50 °C by adding 50 ml of 0.6 M $Co(NO_3)_2 \cdot H_2O$ solution dropwise to 100 ml of 3.2 M NaOH solution under constant stirring. Then, 100 ml of H_2O_2 (50 wt%) was added to the solution drop by drop under constant stirring. The precipitate solution was then filtered, washed with deionized water and dried at 110 °C for 20 h. The dried product was ground and stored in a desiccator as fresh sample.

2.2. Characterization techniques

TPR studies were performed in a fixed-bed reactor. A 25 ml min^{-1} flow of 10% H_2 in Ar was used to reduce the oxidized samples in the TPR experiments. The rate of hydrogen consumption in the experiment was monitored by a thermal conductivity detector (TCD) in the case of

1011-372X/03/0300-0063/0

raising the sample temperature from room temperature (RT) to 500 °C at a constant rate of 10 °C min^{-1}.

X-ray diffraction (XRD) analyses of the samples were carried out using a Siemens D500 diffractometer. The patterns were obtained with CuKα1 radiation ($\lambda = 1.5405$ Å) at a scanning speed of $2\theta = 2^\circ$ min^{-1}.

2.3. In situ FTIR study

A self-supporting wafer (1.3 cm in diameter) was prepared by compressing an 80 mg sample that was mounted in a self-designed high-temperature IR quartz cell with a KBr window. A set of stainless steel gas lines was built and connected to the cell to allow *in situ* measurement of spectra of CO and CO/O_2 probe gases. Prior to adsorption of the probe gases, the wafer was first pretreated in vacuum ($<10^{-4}$ torr) at 500 °C for 30 min and then cooled to the desired temperature. At each temperature, the background spectrum was recorded and was subtracted from the sample spectrum obtained at the same temperature.

3. Results and discussion

3.1. Characterization of cobalt oxides

In order to prepare and characterize cobalt oxides, three oxide derivatives—CoO(OH), Co_3O_4 and CoO—from CoO_x were prepared by controlled hydrogen reduction in TPR to 170, 230 and 300 °C (designated as R-170, R-230 and R-300), respectively.

Figure 1 shows the TPR profiles of a series of cobalt oxide derivatives. Slight variations show the reductive property of these species. The reductive signals (labeled as R_1, R_2, R_3 and R_4) of CoO_x in TPR proceed in four consecutive steps at 150, 225, 260 and 425 °C, respectively. The three latter peaks are merged together. However, the relative area of the four peaks can be determined by means of deconvolution, and the relative area (dashed lines) of R_1, R_2, R_3 and R_4 are 0.20, 1.0, 1.8 and 6.4, respectively. Based on the following equations, the result of comparing the calculated values with the theoretical values (3, 1, 2 and 6, respectively) proves that CoO_x consists of a small amount of CoO_2:

$$2CoO_2 \cdot H_2O + H_2 \longrightarrow 2CoO(OH) + 2H_2O \quad (1)$$

$$6CoO(OH) + H_2 \longrightarrow 2Co_3O_4 + 4H_2O \quad (2)$$

$$Co_3O_4 + H_2 \longrightarrow 3CoO + H_2O \quad (3)$$

$$CoO + H_2 \longrightarrow Co + H_2O \quad (4)$$

Except for the R_1 peak at 150 °C, the TPR profile of the R-170 sample is very similar to that of the CoO_x sample. The disappearance of the R_1 peak for the R-170 sample proves that a pure CoO(OH) species exists at 170 °C reduction. Also, the disappearance of the R_1 and R_2 peaks for the R-230 sample proves that a pure Co_3O_4 species exists at 230 °C reduction. The R-300 sample shows only a single peak at 425 °C. This peak therefore is assigned to the reduction of CoO.

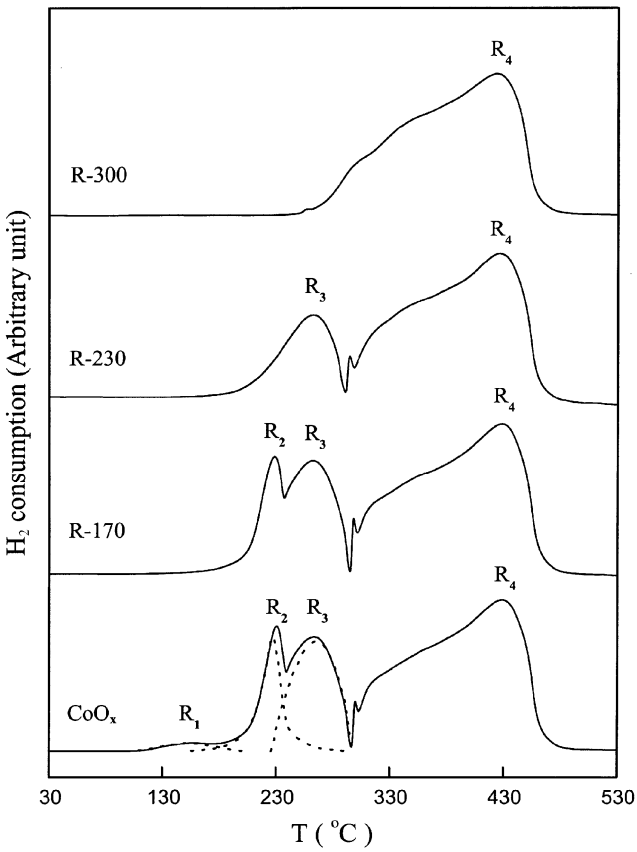

Figure 1. TPR characterization for a series of cobalt oxide derivatives.

Figure 2 shows the XRD patterns of the cobalt oxide derivatives. The results show that the CoO_x and R-170 samples are similar to each other. Both CoO_x and R-170 (CoO(OH)) have a hexagonal structure. The XRD pattern clearly implies that CoO_x undergoes changes in its composition and structure at a reduction temperature above 230 °C. The R-230 sample has a spinel structure, Co_3O_4, and the R-300 sample has a face-centered cubic (f.c.c.) structure, CoO.

3.2. In situ FTIR study

Infrared spectroscopy coupled with probe molecule adsorption is a sensitive technique for investigations of the properties of solid surfaces. We have carried out *in situ* measurements of infrared spectra of CO and CO/O_2 adsorption on the surface of the cobalt oxides. Figures 3 and 4 show the FTIR spectra of the CoO_x and R-230 samples for CO adsorbed under a CO pressure of 30 torr and at different temperatures. (The spectra of R-170 are identical to CoO_x and the spectra of R-300 are identical to R-230, and so only the spectra of CoO_x and R-230 are shown.) The spectra (figure 3) of CoO_x contain bands at 2118, 2172 and 2355 cm^{-1} between

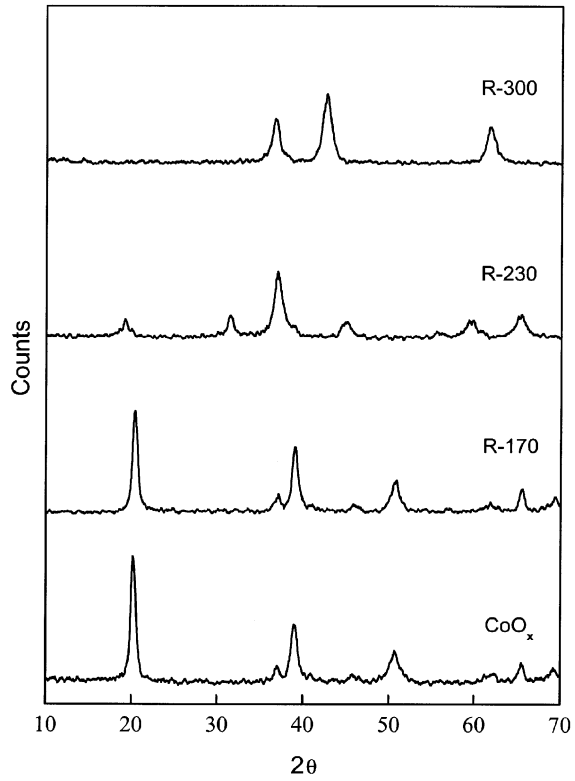

Figure 2. XRD characterization for a series of cobalt oxide derivatives.

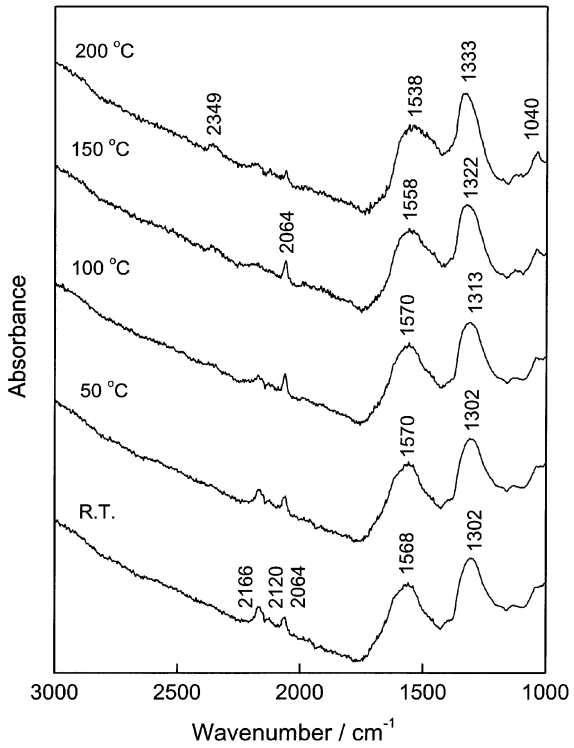

Figure 4. *In situ* FTIR spectra of R-230 (Co_3O_4) for 30 torr CO adsorbed at various temperatures.

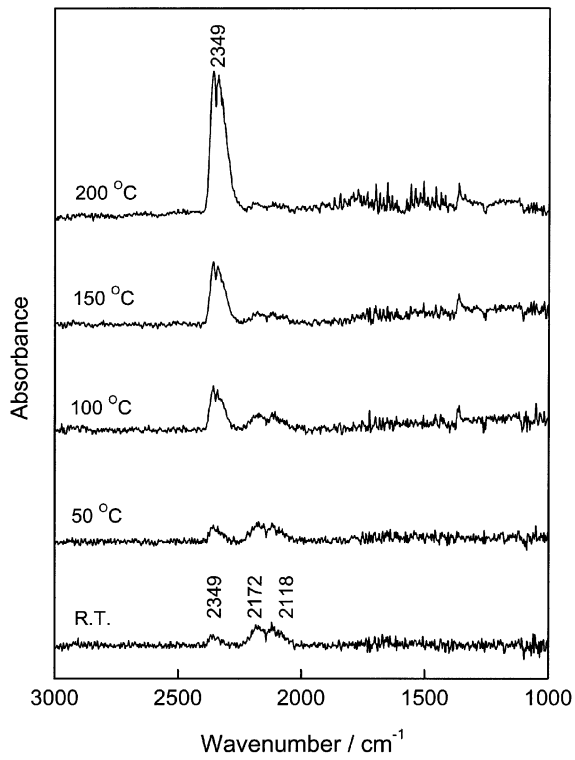

Figure 3. *In situ* FTIR spectra of CoO_x for 30 torr CO adsorbed at various temperatures.

RT and 200 °C. The bands at 2118 and 2172 cm^{-1} might be caused by gaseous CO, which suggests a weak adsorption of CO on the surface of CoO_x:

$$CO + * \Leftrightarrow *-CO \quad (5)$$

where $*$ denotes an adsorption site on the CoO_x surface. The band at 2355 cm^{-1} has been attributed to the ν_3 asymmetric stretch of physisorbed CO_2, being linearly bound to the cation by ion–induced dipole interaction [24,25]. The effect of the temperature up to 200 °C on CO adsorption for the CoO_x sample has been studied. It is noticed that the intensity of the ν_3 band increases in proportion to the temperature. This observation may therefore result from a partial reduction of CoO_x by CO. The weakly bound active oxygen ($*$–O_2) on the CoO_x surface can easily be "swept out" simultaneously by the weakly adsorbed CO to produce CO_2 through the following reaction:

$$*-O_2 + 2*-CO \longrightarrow 2CO_2 + 3* \quad (6)$$

The thermal treatment clearly affects the mobility of the active oxygen. The higher the temperature the more mobile the active oxygen becomes. And of course, the oxidation of CO also becomes easier.

The spectra (figure 4) of R-230 (Co_3O_4) contain bands at 1040, 1300–1330, 1540–1570, 2064, 2120, 2166 and 2355 cm^{-1}. However, no IR absorption is observed at a frequency near the asymmetric stretch of physisorbed CO_2 up to 100 °C. When the system was evacuated after RT exposure to 30 torr CO, the bands at 2120

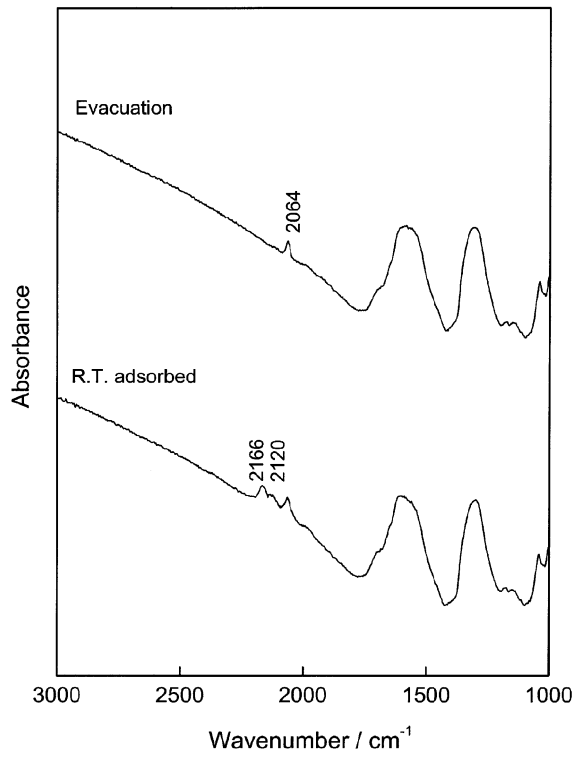

Figure 5. *In situ* FTIR spectra of R-230 (Co_3O_4) for 30 torr CO adsorbed at room temperature for 10 min, and after the system was evacuated.

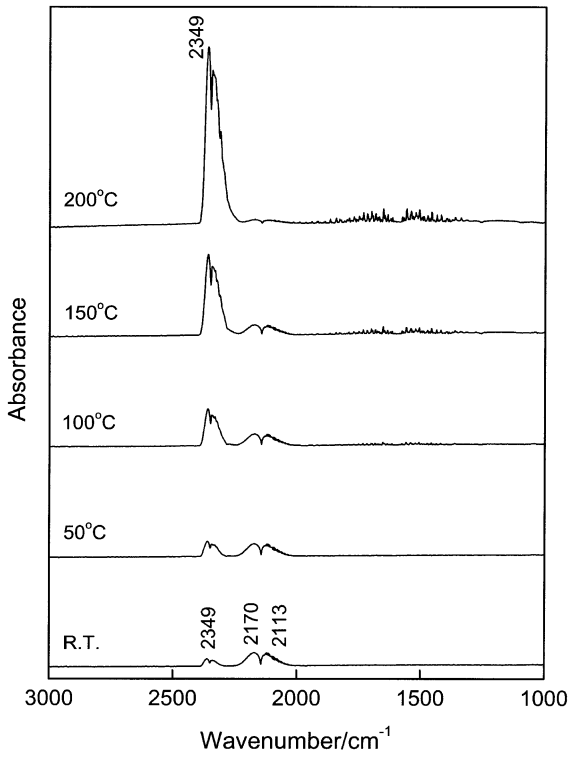

Figure 6. *In situ* FTIR spectra of 30 torr CO and 30 torr O_2 co-adsorption on CoO_x at various temperatures.

and 2166 cm^{-1} disappeared (figure 5). This means that the desorbed bands might be caused by weakly bound species. According to the literature [26,27], the bands at 1040, 1300–1330 and 1540–1570 cm^{-1} are the characteristic vibrations of surface bidentate carbonate species (ν_sCOO, ν_{as}COO and νC=O, respectively) that are formed through the interaction of lattice oxygen ($*$–O_L) of Co_3O_4 with adsorbed CO:

$$*-O_L + *-CO \longrightarrow *-\text{carbonate} \qquad (7)$$

The band near 2064 cm^{-1} may be affected by the linearly adsorbed CO. When the temperature increased, the band at 2064 cm^{-1} also increased gradually, reaching its strongest intensity at 150 °C. On heating to 200 °C, this band became weaker due to the desorption of adsorbed CO. The bands at 2120 and 2166 cm^{-1} are assigned to dicarbonyl (ν_sCO and ν_{as}CO) species [28]. After the CO-adsorbed material was heated, the intensities decreased gradually and almost disappeared at 150 °C due to the reaction with the weakly bound active oxygen on Co_3O_4, but the formation of CO_2 (the band near 2355 cm^{-1}) appeared gradually. Comparing the formation of CO_2 with the CoO_x sample, it can be seen that CoO_x has a higher active oxygen content than does Co_3O_4. When the temperature increased, the ν_{as}COO and νC=O bands shifted respectively from 1300 to 1333 cm^{-1} and from 1568 to 1538 cm^{-1}. Apparently, the slight change of the band positions indicates the influence of the reaction of CO with the active oxygen on Co_3O_4.

The influence of CO/O_2 co-adsorption was studied by testing the CoO_x and R-230 (Co_3O_4) samples. In the CO/O_2 adsorption experiments (figures 6 and 7), 30 torr CO was first introduced into the chamber at room temperature giving rise to absorption bands (figures 3 and 4), and then 30 torr O_2 was introduced. The spectrum of CO/O_2 co-adsorption (figure 6) is similar to CO adsorption on CoO_x (figure 3). As O_2 was introduced and the temperature was increased, no obvious changes occurred to the bands. This means that the CO oxidation on the CoO_x sample comes from the weakly bound active oxygen rather than from adsorbed oxygen or lattice oxygen.

A significant band near 2355 cm^{-1} appeared as O_2 was introduced to the R-230 (Co_3O_4) sample (figure 7) at RT, which was different from CO/O_2 co-adsorption on CoO_x. This indicated that physisorbed CO_2 was formed as soon as O_2 was introduced over the CO pre-adsorbed on Co_3O_4 and the intensity was significant at RT. After 15 min at RT the adsorbed CO disappeared due to the complete oxidation of CO by O_2. It should be noted that the intensity of the bands near 1300 and 1568 cm^{-1} decreased quickly upon formation of physisorbed CO_2 but still remained at the same intensity under various conditions. This behavior indicates that most of the CO_2 was formed during CO adsorption probably due to the interaction of bidentate carbonate with oxygen. The consumed lattice oxygen ($*$–O_L) may be restored through adsorption of oxygen molecules on

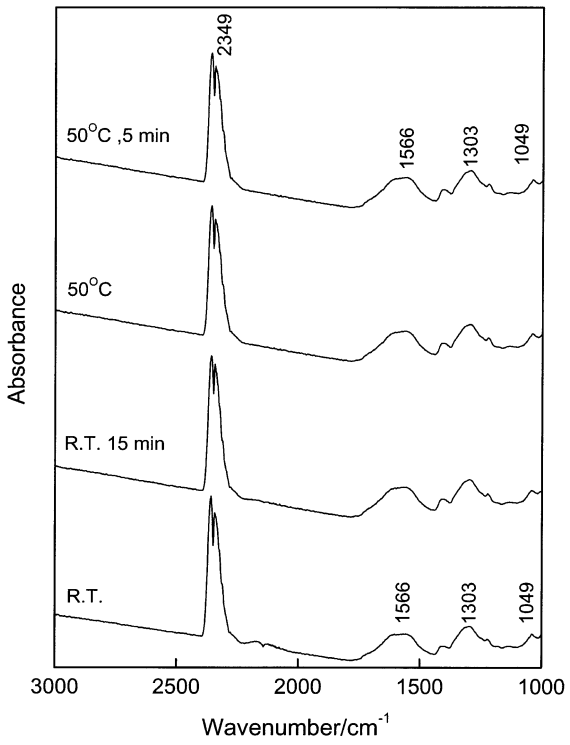

Figure 7. *In situ* FTIR spectra of 30 torr CO and 30 torr O_2 co-adsorption on R-230 (Co_3O_4) at various temperatures.

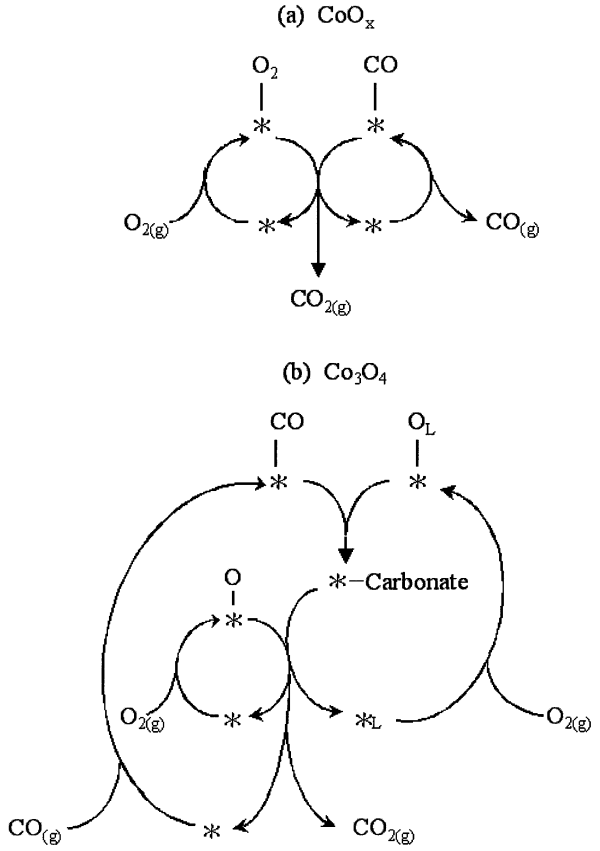

Figure 8. Proposed reaction models suggested for CO/O_2 co-adsorption on cobalt oxides: (a) CoO_x and (b) R-230 (Co_3O_4).

the resulting vacancy ($*_L$):

$$*-\text{carbonate} + *-O \longrightarrow CO_2 + * + *_L \quad (8)$$

$$2*_L + O_2 \longrightarrow 2*-O_L \quad (9)$$

Figure 8 summarizes the two sets of reaction mechanisms proposed for CO/O_2 co-adsorption over CoO_x and Co_3O_4. The major difference between these two mechanisms lies in the types of surface oxygen involved. In the absence of lattice oxygen, the weakly adsorbed CO on CoO_x has to be oxidized by the weakly bound active oxygen ($*–O_2$). The $*–O_L$ on Co_3O_4 is more active than $*–O_2$ and may form an intermediate, that is, bidentate carbonate, which could oxidize CO to produce CO_2.

4. Conclusion

A mixed cobalt oxide, CoO_x, was prepared by the precipitation–oxidation method and further refined to other pure cobalt oxides with a controlled hydrogen reduction. Based on the characterizations of the cobalt oxides using TPR and XRD in this study, and the CO and CO/O_2 co-adsorption *in situ* FTIR study, we propose that: (i) the reduction of CoO_x in TPR proceeds in consecutive steps; and (ii) the variation in oxidation of CO is interpreted with a mechanism of two kinds of oxygen species, i.e., $*–O_2$ on the CoO_x surface and $*–O_L$ on the surface of Co_3O_4 spinel structure.

Acknowledgment

The authors acknowledge the financial support for this study by the National Science Council and Academia Sinica of the Republic of China.

References

[1] D.G. Castner, Ph.R. Watson and I.Y. Chan, J. Phys. Chem. 93 (1989) 3188.
[2] Y.J. Mergler, A. van Aalst, J. van Delft and B.E. Nieuwenhuys, J. Catal. 161 (1996) 310.
[3] Y.J. Mergler, A. van Aalst, J. van Delft and B.E. Nieuwenhuys, Appl. Catal. B 10 (1996) 245.
[4] K. Omata, T. Takada, S. Kasahara and M. Yamada, Appl. Catal. A 146 (1996) 255.
[5] Y.J. Mergler, J. Hoebink and B.E. Nieuwenhuys, J. Catal. 167 (1997) 305.
[6] J. Jansson, J. Catal. 194 (2000) 55.
[7] H. Hamada, Y. Kintaichi, M. Inaba, M. Tabata, T. Yoshinari and H. Tsuchida, Catal. Today 29 (1996) 53.
[8] A. Torncrona, M. Skoglundh, P. Thormahlen, E. Fridell and E. Jobson, Appl. Catal. B 14 (1997) 131.
[9] D. Pietrogiacomi, S. Tuti, M.C. Campa and V. Indovina, Appl. Catal. B 28 (2000) 43.
[10] E. Garbowski, M. Guenin, M.C. Marion and M. Primet, Appl. Catal. 64 (1990) 209.

[11] A.S.K. Sinha and V. Shankar, J. Chem. Eng. Biochem. Eng. 52 (1993) 115.
[12] F. Lichtenberg and K. Kleinsorgen, J. Power Sources 62 (1996) 207.
[13] E. Antolini and E. Zhecheva, Mater. Lett. 35 (1998) 380.
[14] T.J. Boyle, D. Ingersoll, T.M. Alam, C.J. Tafoya, M.A. Rodriguez, K. Vanheusden and D.H. Doughty, Chem. Mater. 10 (1998) 2770.
[15] H. Yamaura, J. Tamaki, K. Moriya, N. Miura and N. Yamazoe, J. Electrochem. Soc. 144 (1997) L158.
[16] H. Yamaura, K. Moriya, N. Miura and N. Yamazoe, Sensors Actuators B65 (2000) 39.
[17] E. Gulari, C. Güldür, S. Srivannavit and S. Osuwan, Appl. Catal. A 182 (1999) 147.
[18] D.R. Lide, *Handbook of Chemistry and Physics*, 72nd edition (1991–1992).
[19] R.B. King, *Encyclopedia of Inorganic Chemistry*, Vol. 2 (Wiley, 1994).
[20] R. Van Zee, Y. Hamrick, S. Li and W. Weltner, J. Phys. Chem. 96 (1992) 7247.
[21] M. Elemongy, M. Gouda and Y. Elewady, J. Electroanal. Chem. 76 (1977) 367.
[22] D. Chen Yih-Wen and N.N. Rommel, J. Electrochem. Soc. 131 (1984) 731.
[23] St.G. Christoskova, M. Stoyanova, M. Georgieva and D. Mehandjiev, Mater. Chem. Phys. 60 (1999) 39.
[24] J.W. Ward and H.W. Habgood, J. Phys. Chem. 70 (1966) 1178.
[25] P.A. Jacobs, F.H. Cauwelaert, E.F. Vansant and J.B. Utterhoven, J. Chem. Soc. Faraday Trans. I 69 (1973) 1056.
[26] J. Fujita, A.E. Martell and K. Nakamoto, J. Chem. Phys. 36 (1962) 339.
[27] G.K. Boreskov, Kinet. Katal. 8 (1967) 1020.
[28] V.S. Kamble, N.M. Gupta, V.B. Kartha and R.M. Iyer, J. Chem. Soc. Faraday Trans. 89 (1993) 1143.